Revised geochronology of the Casamayoran South American Land Mammal Age: Climatic and biotic implications

Richard F. Kay*†, Richard H. Madden*, M. Guiomar Vucetich‡, Alfredo A. Carlini‡, Mario M. Mazzoni‡§, Guillermo H. Re¶, Matthew Heizler‖, and Hamish Sandeman**

*Department of Biological Anthropology and Anatomy, Duke University, Durham, NC 27710; ‡Facultad de Ciencias Naturales y Museo, Universidad Nacional de La Plata, La Plata, Argentina; ¶Facultad de Ciencias Exactas y Naturales, Universidad de Buenos Aires, Buenos Aires, Argentina; ‖Department of Earth and Environmental Sciences, New Mexico Institute of Mining and Technology, Socorro, NM 87801; and **Department of Geological Sciences, Queen's University, Kingston, ON, Canada K7L 3N6

Edited by David L. Dilcher, University of Florida, Gainesville, FL, and approved July 21, 1999 (received for review April 20, 1999)

Isotopic age determinations ($^{40}Ar/^{39}Ar$) and associated magnetic polarity stratigraphy for Casamayoran age fauna at Gran Barranca (Chubut, Argentina) indicate that the Barrancan "subage" of the Casamayoran South American Land Mammal "Age" is late Eocene, 18 to 20 million years younger than hitherto supposed. Correlations of the radioisotopically dated magnetic polarity stratigraphy at Gran Barranca with the Cenozoic geomagnetic polarity time scale indicate that Barrancan faunal levels at the Gran Barranca date to within the magnetochronologic interval from 35.34 to 36.62 megannums (Ma) or 35.69 to 37.60 Ma. This age revision constrains the timing of an adaptive shift in mammalian herbivores toward hypsodonty. Specifically, the appearance of large numbers of hypsodont taxa in South America occurred sometime between 36 and 32 Ma (late Eocene–early Oligocene), at approximately the same time that other biotic and geologic evidence has suggested the Southern high latitudes experienced climatic cooling associated with Antarctic glaciation.

mammalian evolution | South America | Eocene | paleontology

The isotopic ages of Eocene mammalian faunas of South America are poorly known: there are no radiometric dates from rock units containing fossil mammals. Two time-successive faunas, the Casamayoran and the Mustersan South American Land Mammal Ages (SALMAs), conventionally are regarded as representing early [55–50 megannums (Ma)] and middle (45–40 Ma) Eocene, respectively. A third, the Divisaderan, found only at one locality, is considered to be late Eocene (1–6). We report newly dated rocks from the Gran Barranca, a cliff south of Lake Colhue Huapi (S45° 42′ 49″, W68° 44′ 16″ in Chubut Province, Argentina) where there occurs an important Cenozoic fossil-mammal succession (Figs. 1 and 2). The Gran Barranca consists of pyroclastic sediments of the Sarmiento Formation, which is subdivided into three members (7, 8). (*i*) The oldest Gran Barranca member contains a fauna upon which is based the Barrancan "subage" of the Casamayoran SALMA, the younger of two subages (Vacan and Barrancan) of the Casamayoran (9). (*ii*) The intermediate Puesto Almendra member contains the type assemblage of the Mustersan SALMA (3). Toward the top of this member occurs an as-yet poorly sampled fauna called the "Astraponotéen plus Supérieur" of Ameghino††, similar faunally to the Tinguiririca fauna of central Chile (10, 11). The Puesto Almendra member is disconformably overlain by basalt flows dated (K–Ar) at 28.8 ± 0.9 Ma (12). (*iii*) The youngest exposed unit is the richly fossiliferous Colhue-Huapi member, which contains a major locality for mammals of the Colhuehuapian SALMA. At Gran Barranca this latter fauna is dated to between 20.5 and 19.1 Ma. (13). Thus, Gran Barranca samples all Eocene through Oligocene SALMAs except possibly the Deseadan. (Mammals of the Deseadan age may occur at the Barranca accompanying stringers of basalt pebbles associated with the initial stages of the erosion of the basalt flows.)

Methods and Results

A stratigraphic interval (75 m) of the Gran Barranca, encompassing the Gran Barranca and Puesto Almendra members and including the Barrancan, Mustersan, and Astraponotéen plus Supérieur faunas, was sampled for radiometric age determination and magnetic polarity stratigraphy. Three $^{40}Ar/^{39}Ar$ dates were obtained from a sample of dark glass-rich pyroclastic tuff, MZ-7 level [stratigraphic levels in the measured composite section of the Sarmiento Formation at the west end of Gran Barranca are staked, labeled, numbered consecutively, and designated MZ by one of the authors of the present paper (M.M.M.)], equivalent to the "steel gray band" (9) within the Gran Barranca member and within the sampled range of the Barrancan fauna (Fig. 1). Bulk plagioclase and glass separates from MZ-7 were analyzed by $^{40}Ar/^{39}Ar$ laser-fusion and step-heating age spectrum methods, respectively. The age spectrum for glass did not yield a plateau age, but climbed to an age of 32.74 ± 0.90 Ma for the final 30% of the released ^{39}Ar (Table 1; Fig. 2 *Upper*). The age gradient for glass suggests argon loss, so the maximum age recorded by the high temperature steps is interpreted to be a minimum age for the glass. Plagioclase was also analyzed by laser fusion (Fig. 2 *Lower*). Seven splits yielded analytically indistinguishable total-fusion ages with a weighted mean of 36.01 ± 0.44 Ma (Table 2). Given the fine-grained nature of the plagioclase, we cannot rule out xenocrystic contamination during postdepositional reworking and/or from the vent during eruption. Assuming no argon loss, the plagioclase age is interpreted to represent a maximum age. On the basis of these results, the age range for the volcanic eruption producing the MZ-7 tuff is between 32.7 and 36.0 Ma. A whole rock sample from MZ-7 was analyzed with the total fusion $^{40}Ar/^{39}Ar$ method by a second laboratory, yielding an age of 38.1 ± 3.0 Ma (Table 3). The whole-rock data suggest that the true age is closer to the plagioclase than to the glass age (i.e., nearer 36 Ma).

Rock samples were collected for paleomagnetic study (five samples for each site from MZ-1 to MZ-16) through the Gran Barranca and Puesto Almendra members (Fig. 1). The sampling interval between sites averaged 10 meters. From each sample, two specimens were obtained and the magnetic susceptibility, intensity,

This paper was submitted directly (Track II) to the PNAS office.

Abbreviations: Ma, megannum, 1 million years in the radioisotopic time scale; GPTS, geomagnetic polarity time scale; MZ, Mazzoni stratigraphic level; SALMA, South American Land Mammal Age.

†To whom reprint requests should be addressed. E-mail: Rick_Madden@baa.mc.duke.edu.

§Deceased October 1, 1999.

††Bond, M., Reguero, M. A. & Vizcaino, S. F., *Boletin de Resumenes, XIII Congresso Brasileiro de Paleontologia y I Simposio de Paleontólogia do Cone Sul,* Universidade do Vale do Rio dos Sinos, Sao Leopoldo, Brasil, September 19–26, 1993, p. 93 (abstr.).

The publication costs of this article were defrayed in part by page charge payment. This article must therefore be hereby marked "*advertisement*" in accordance with 18 U.S.C. §1734 solely to indicate this fact.

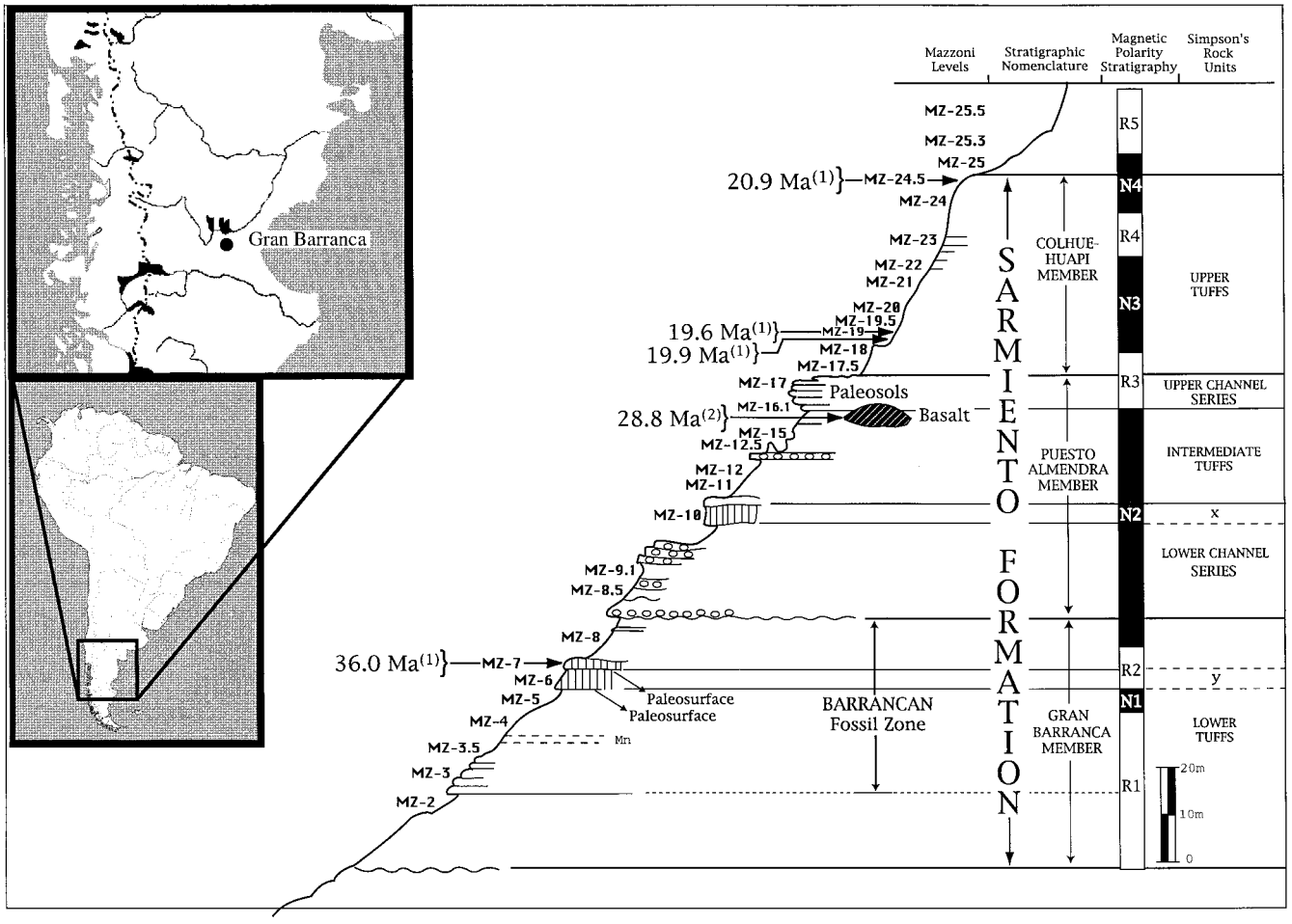

Fig. 1. Stratigraphic profile of the west end of the Gran Barranca, south of Lake Colhué-Huapí, Chubut Province, Argentina, indicating MZ levels, lithostratigraphy, stratigraphic nomenclature (7, 8), dated levels, magnetostratigraphy, Simpson's informal stratigraphic terminology, and the Barrancan faunal zone. The profile on which the figure is based is 0.5 km east of Cifelli's (9) Section I. MZ levels sampled for magnetic polarity stratigraphy, radioisotopic dating, lithostratigraphy, and phytolith stratigraphy. Radioisotopic dates are from this paper and refs. 11, 12, and 44. $^{40}Ar/^{39}Ar$ and ^{40}K–^{40}Ar dates are given in Ma.

declination, and inclination of the natural remnant magnetization were measured by using a 2-G cryogenic magnetometer at the University of Buenos Aires. Half of the specimens were subjected to demagnetization in 15 incremental steps to a maximum temperature of 700°C in a Schonstedt (Kearneysville, WV) SSM2 furnace. Magnetic susceptibility was measured after each heating step to determine possible changes in magnetic mineralogy. The remaining specimens were subjected to alternating field demagnetization. Up

Table 1. Furnace argon isotopic results for MZ-7 glass

Step	Temp, °C	$^{40}Ar/^{39}Ar$	$^{37}Ar/^{39}Ar$	$^{36}Ar/^{39}Ar$ ($\times10^{-3}$)	$^{39}Ar_K$ ($\times10^{-15}$ mol)	K/Ca	$^{40}Ar^*$, %	^{39}Ar, %	Age, Ma	$\pm1\ \sigma$, Ma
A	550	10385	0.2738	35070	0.132	1.9	0.2	0.4	32	504
B	600	134.3	0.5938	435.1	1.03	0.86	4.3	3.1	8.4	1.5
C	650	69.96	0.6300	201.8	2.71	0.81	14.8	10.3	14.96	0.51
D	700	52.46	0.6468	131.1	2.43	0.79	26.2	16.7	19.81	0.53
E	730	53.10	0.7097	121.3	6.31	0.72	32.6	33.5	24.90	0.32
F	760	47.85	0.7493	96.78	4.84	0.68	40.3	46.3	27.75	0.27
G	800	53.06	0.7971	107.3	6.25	0.64	40.3	62.9	30.75	0.29
H	830	59.22	0.8182	125.6	5.39	0.62	37.4	77.2	31.83	0.34
I	870	71.23	0.8627	164.1	4.11	0.59	32.0	88.1	32.74	0.45
J	900	118.9	0.9004	329.1	2.40	0.57	18.3	94.5	31.17	0.76
K	950	318.3	0.9827	1007.8	1.39	0.52	6.5	98.2	29.6	2.6
L	1000	1302.7	0.8560	4331	0.688	0.60	1.8	100.0	33.0	14.0
Total gas age					37.7	0.67			27.3	2.5

MZ-7 glass, sample mass = 19.73 mg, *J* (radiation parameter for neutron flux) = 0.0008025, Laboratory sample 8955–01. $^{40}Ar^*$ indicates radiogenic ^{40}Ar.

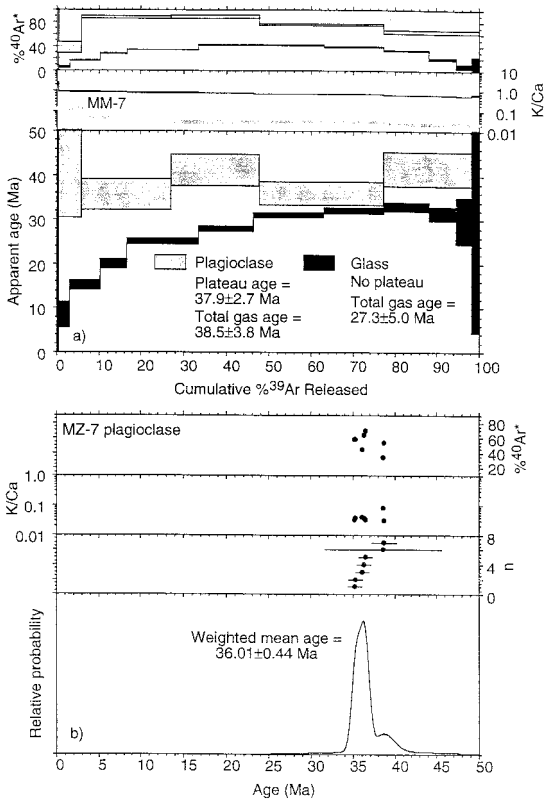

Fig. 2. Results of $^{40}Ar/^{39}Ar$ dating analyses for MZ-7 tuff horizon within the Barrancan faunal interval at Gran Barranca. (*Upper*) Age spectra, K/Ca, and radiogenic yield diagrams for double-vacuum furnace-heated MZ-7 plagioclase and glass. (*Lower*) Probability distribution, K/Ca, and radiogenic yield diagrams for MZ-7 plagioclase laser fusion data.

to 20 demagnetization stages were applied up to a maximum field of 130 mT by using a 2-G magnetometer. Magnetic mineralogy was analyzed by using isothermal remnant magnetization, subjecting specimens to magnetic fields that reached values, in successive steps, of up to 2500 mT. The results were analyzed with MAG88 software (14); magnetic signatures were plotted on an orthogonal diagram (15). Components of the natural remnant magnetization were identified by principal components analysis (16). After isolating the characteristic remnant magnetization of each specimen, the directions were averaged and virtual geomagnetic poles were calculated for each site (17). Normal polarity was assigned to those sites with polarity between 0° and 90°, and reverse polarity was assigned to sites with polarity between 90° and 180° (see Fig. 1).

The lower levels (MZ-1 through MZ-4) are reversed in polarity (local reversed zone R1). Polarity is normal in MZ-5 (designated N1 in Fig. 1), but is again reversed at MZ-6 and MZ-7 (R2). MZ-6 samples a thick white tuff that is the prominent and continuous "marker" bed recognized by G. G. Simpson during his expedition to Gran Barranca in 1930 (9). Samples MZ-8 through MZ-16 across the upper Gran Barranca member and through the disconformity at the base of the Puesto Almendra member are again normal in polarity (N2). The plagioclase date (36.01 ± 0.44 Ma) for level MZ-7 indicates the reversed polarity interval (R2) and correlates with either Subchron C16n.1r (35.526 to 35.685 Ma) or Chron 16r (36.341 to 36.618 Ma) of the geomagnetic polarity time scale (GPTS) (18). Barrancan faunal levels are found in the MZ-6 and MZ-7 reversed polarity interval as well as in the normal (N1) and reversed interval (R1) below and the normal interval (N2) above. Thus, Barrancan faunal levels at the Gran Barranca date to within the magnetochronologic interval from 35.34 to 36.62 Ma or from 35.69 to 37.60 Ma.

Upward revision of the Barrancan subage to the late Eocene creates a temporal gap within the Eocene record of mammalian evolution in Patagonia (Fig. 3). If the Riochican SALMA is Paleocene (19, 20), only the Vacan subage of the Casamayoran is

Table 2. Furnace argon isotopic results for MZ-7 plagioclase

Step	Temp, °C	$^{40}Ar/^{39}Ar$	$^{37}Ar/^{39}Ar$	$^{36}Ar/^{39}Ar$ ($\times10^{-3}$)	$^{39}Ar_K$ ($\times10^{-15}$ mol)	K/Ca	$^{40}Ar^*$, %	^{39}Ar, %	Age, Ma	±1 σ, Ma
A	700	82.37	4.689	177.9	0.068	0.11	36.6	5.9	43.3	6.5
B	900	28.34	12.52	16.22	0.246	0.041	86.5	27.1	35.4	1.7
C	1100	32.52	19.87	19.68	0.241	0.026	86.8	47.9	41.0	1.8
D	1300	33.21	19.35	34.09	0.341	0.026	74.1	77.4	35.8	1.3
E	1650	45.16	24.43	63.22	0.262	0.021	62.8	100.0	41.3	1.9
Total gas age					1.16	0.033			38.5	1.9
Preferred age					1.16	0.033		100.0	37.9	2.7**

MZ-7 plagioclase, sample mass = 4.16 mg, J = 0.0008025, Laboratory sample 8955-02. For calculation of both ages, n = 5. For preferred age from steps A–E, mean standard weighted deviation (MSWD) = 2.87 (outside of 95% confidence interval). **, 2 σ error.

Table 3. Laser argon isotopic results for MZ-7 plagioclase

Step	$^{40}Ar/^{39}Ar$	$^{37}Ar/^{39}Ar$	$^{36}Ar/^{39}Ar$ ($\times10^{-3}$)	$^{39}Ar_K$ ($\times10^{-15}$ mol)	K/Ca	$^{40}Ar^*$, %	Age, Ma	±1 σ, Ma
06	41.84	15.86	63.42	0.341	0.032	58.1	35.26	0.51
05	41.95	14.01	63.00	0.349	0.036	58.2	35.34	0.46
04	56.79	13.20	111.1	0.385	0.039	44.0	36.15	0.52
07	39.31	14.00	51.69	0.272	0.036	63.9	36.34	0.53
09	36.43	15.80	42.08	0.289	0.032	69.2	36.54	0.46
08	79.53	6.180	180.0	0.034	0.083	33.7	38.6	6.7
03	49.56	16.21	81.49	0.162	0.03	53.9	38.7	1.2
Weighted mean age					0.041 ± 0.018		36.01	0.44**

MZ-7 plagioclase sample masses = 1–3 mg, J = 0.0008025, Laboratory sample 8955. Isotopic ratios are corrected for blank, radioactive decay, and mass discrimination, not corrected for interfering reactions. Individual analyses show analytical error only; plateau, preferred, and total gas age errors includes error in J and irradiation parameters. K/Ca = molar ratio calculated from reactor-produced $^{39}Ar_K$ and $^{37}Ar_{Ca}$. For calculation of the weighted mean age (n = 7), mean standard weighted deviation (MSWD) = 1.92. **, 2 σ error.

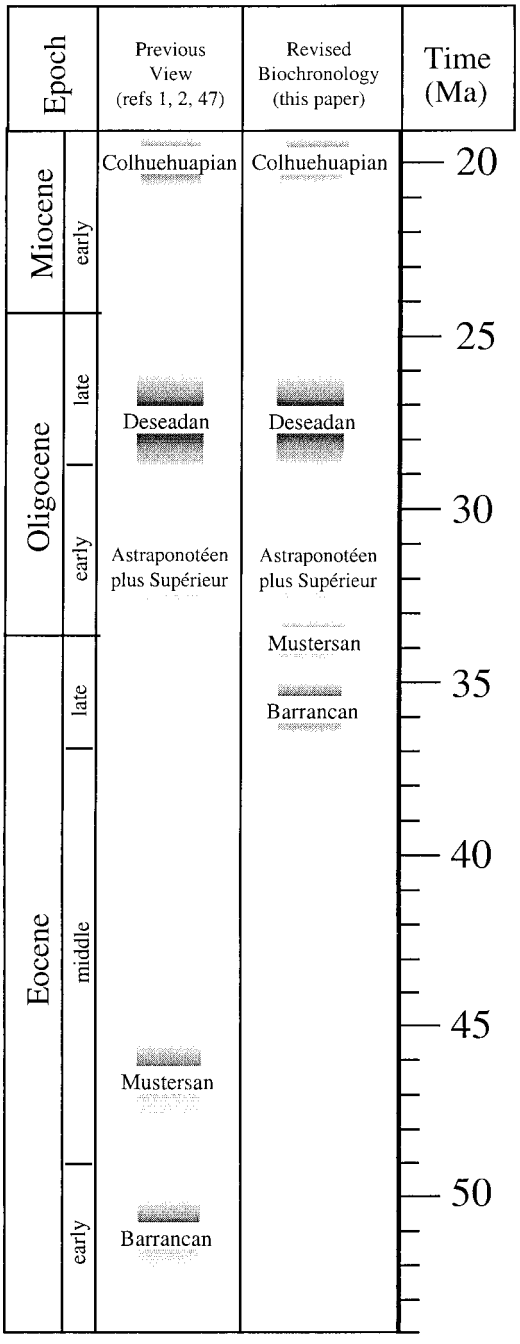

Fig. 3. Revised time scale for middle Cenozoic mammalian faunas of South America. *Left*, column indicating epoch boundaries, following Berggren *et al.* (18). *Center*, column giving previous view of mammalian biochronology of SALMAs (1, 2, 44). *Right*, column shows revision as presented here. Temporal scale in Ma.

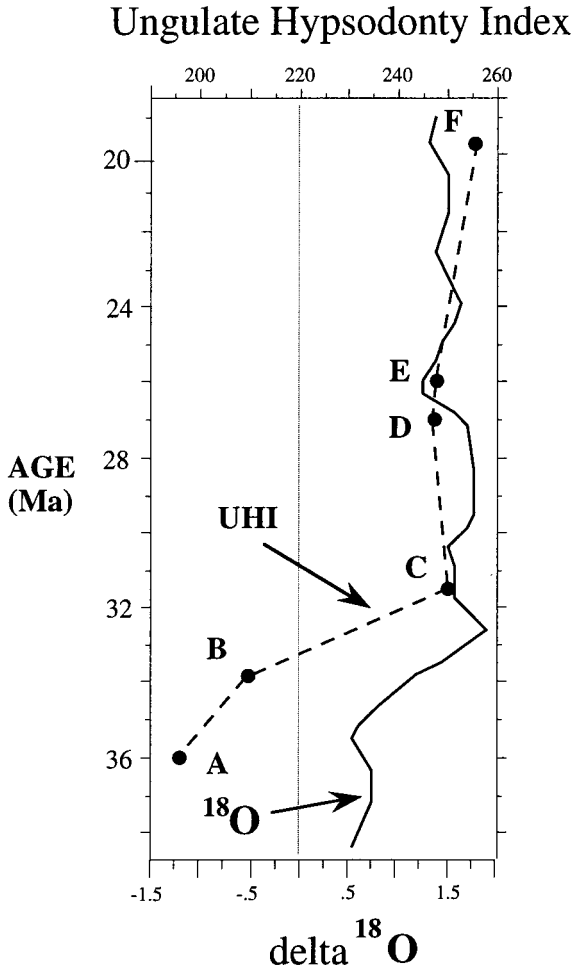

Fig. 4. Change in sea-surface temperatures in the South Atlantic Ocean and hypsodonty in ungulate mammals between 39 and 19 Ma. Solid line, foraminiferal ^{18}O isotope data from K. G. Miller (personal communication), calibrated to the GPTS of Berggren *et al.* (18). Hypsodonty is expressed as an ''Ungulate Hypsodonty Index'' (UHI), the weighted sum of bunodont (weight = 1), lophodont (weight = 2), and hypsodont (weight = 3), taxa. If all taxa are bunodont, UHI = 100; if all are hypsodont, UHI = 300. Faunas: A, Barrancan; B, Mustersan; C, Tinguiririca and Astraponotéen plus Supérieur; D, Deseadan of Patagonia; E, Salla, Deseadan; and F, Colhuehuapian.

left to fill the entire early and middle Eocene of the Patagonia fossil mammal record. The question of whether the Riochican really falls in the Paleocene is unresolved: there are no radiometric dates that bear directly on its age; they merely indicate that Riochican faunas are younger than early Paleocene (i.e., <63 Ma) (19, 20). The revised age of the Barrancan also compresses the temporal interval into which the Mustersan and Astraponotéen plus Supérieur faunas must fit (Fig. 3). These two intervals at Gran Barranca must be younger than about 35.3 Ma (the youngest possible age for the Barrancan) and older than 28.8 Ma [a dated basalt overlies them (12)]. If the Astraponotéen plus Supérieur fauna at the Gran Barranca is contemporaneous with the Chilean Tinguiririca fauna dated at about 31.5 Ma (11, 21), with which it shares a number of genera (10, 11, 21), then the Mustersan (not yet dated) should fall between 32 and 35 Ma.

Discussion

Our revised age estimates for the middle Cenozoic SALMAs of Patagonia help resolve an apparent discrepancy between the age of placental and marsupial mammals from the La Meseta Formation of Seymour (Marambio) Island and provide an additional constraint on the timing of faunal exchange between South America and Antarctica. Published locality and occurrence data indicate a single faunal assemblage in the La Meseta Formation comprising both placental and marsupial mammals (22). Case and others (23, 24) have argued that the marsupials are late Eocene (about 40 Ma), based on the age of the associated marine invertebrates. Marenssi *et al.* (22) point out that morphological similarities between the placental mammals from Seymour Island and those from Patagonia argue for a Casamayoran, or more broadly, a Riochican through

Mustersan age correlation—late Paleocene through middle Eocene in the conventional correlation scheme (1, 20). Our revised late-Eocene age for the Barrancan (Casamayoran) of Patagonia therefore gives the placental mammals consistency with all other faunal components in indicating a late Eocene age for the La Meseta Formation (25–28). Furthermore, mammalian faunal similarities between southern South America and the Antarctic Peninsula are consistent with terrestrial faunal exchange having continued into the late Eocene, in agreement with other evidence that constrains the age of the opening of the Drake Passage to between 22 and 32 Ma (29).

The South American continental biotic record can now be temporally calibrated against a record of climatic change derived from marine sediments of the late Eocene through Oligocene ages. What emerges is a close correspondence between climate change in the marine sedimentary record of the South Atlantic and change in continental palaeofloras and palaeomammals in Patagonia.

Evidence places the earliest large ice sheets in Antarctica at *ca.* 33 Ma, i.e., the earliest Oligocene (30). The climate in the late Eocene-to-Miocene in Antarctica and Patagonia changed in three major steps (31): (*i*) the late Eocene (34.5–36.5 Ma; Barrancan), when relatively warm conditions prevailed, but glacier formation was initiated; (*ii*) the late Eocene-early Oligocene (28.5–34.5 Ma; Mustersan and Astraponotéen plus Supérieur), characterized by the transition from relatively warmer to cooler conditions coinciding with glacial intensification and sea-level fall; and (*iii*) the late Oligocene-early Miocene (22–28.5 Ma; Deseadan, pre-Colhuehuapian), when large-scale glaciation began to dominate Antarctica.

Atmospheric general circulation model sensitivity experiments indicate that Eocene ocean cooling may have been accompanied by four responses in Patagonia: (*i*) a decrease in mean annual precipitation, (*ii*) a decrease in mean annual temperature, (*iii*) an increase in seasonal temperature amplitude, and (*iv*) a decrease in the mean temperature of the coldest month (32).

The phytolith stratigraphy of the Sarmiento Formation at Gran Barranca (33) is in general agreement with the pattern of changes predicted by the climate model. During the Barrancan-to-Deseadan interval, the proportion of palm (globulolite) cystoliths decreases, presumably in response to the cooling trend. An increase in the proportion of grass phytoliths and the replacement of panicoid by festucoid grasses also suggests cooling and drying conditions.

From the Barrancan through the Deseadan (between about 36 and 25 Ma) in Patagonia, mammalian niche structure was transformed in ways that suggest a strong faunal response to climate change. At least six families of archaic southern ungulates went extinct: Oldfieldthomasiidae, Archaeohyracidae, Henricosborniidae, Didolodontidae, Trigonostylopidae, and Notostylopidae (3). Except for the archaeohyracids, these families are predominantly species that have low-crowned cheek teeth. Other ungulate families with high-crowned cheek teeth, including Hedgetotheriidae and Mesotheriidae, make their initial appearance in this interval.

The appearance of large numbers of hypsodont taxa in South America occurred after 36 Ma and before 32 Ma, and coincides with accelerated cooling of ocean surface temperatures in the southern hemisphere between 36 and 33 Ma (34, 35) (Fig. 4). Evidence suggests a causal link between climate variables influencing vegetation and the teeth of herbivorous mammals. For example, the proportion of hypsodont species of sigmodontine rodents is significantly correlated with the four climate variables used in the climate sensitivity experiment (Fig. 5). However, the adaptive significance of hypsodonty is more subtle. Is it the physical properties of plants that selected for increased mammalian crown height or is it the exogenous grit that adheres to plant parts?

Hypsodonty in mammalian herbivores prolongs the life of the dentition (36). The timing and adaptive significance of the rise of hypsodonty among mammalian herbivores are poorly understood (2, 4, 37–41). Hypsodonty may maintain the functional

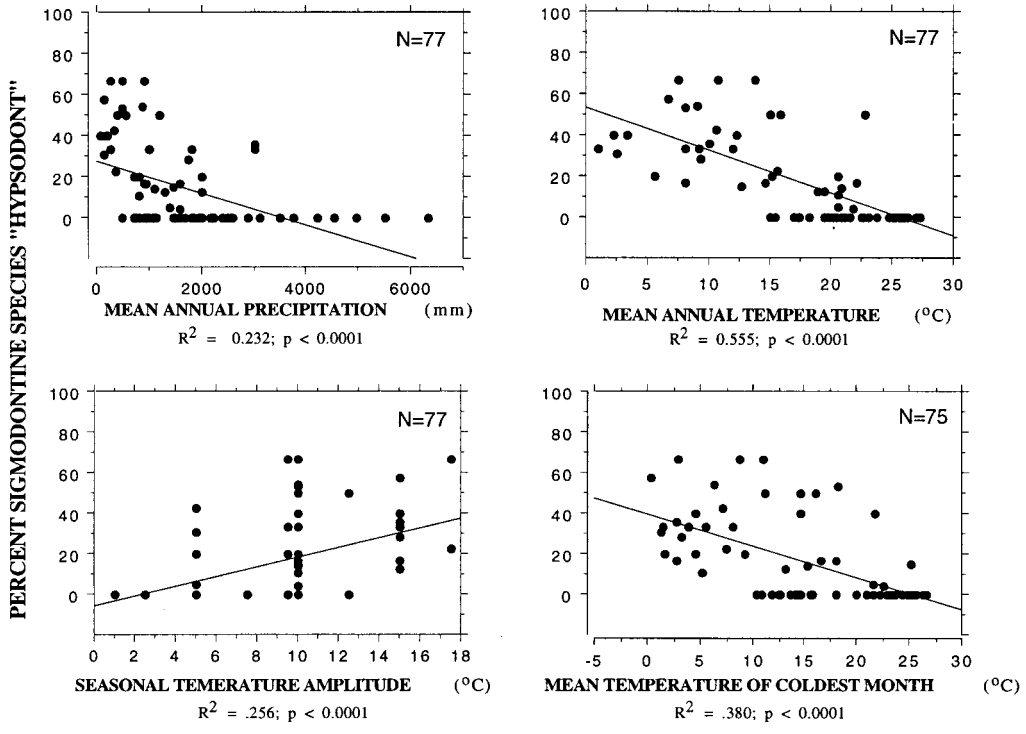

Fig. 5. Percentage of hypsodont species of extant sigmodontine rodents at 75–77 modern South American localities vs. mean annual precipitation, mean annual temperature, seasonal temperature amplitude, and mean temperature of the coldest month. Meterological data from the nearest agrometeorological station (45). Species scored as hypsodont if cheek tooth crown height is greater than in typical oryzomyins (46, 47). Of 197 species of Sigmodontinae, 141 species could be classified, of which 24 are hypsodont.

life of cheek teeth in herbivores whose teeth wear rapidly because of dietary grit. Therefore, hypsodonty may be a coevolutionary response to the evolution of silica phytoliths in plant (especially grass) leaves, or to increases in exogenous dietary grit in the form of wind-blown dust, or to both factors[‡‡]. The oldest evidence for grasses in southern South America is in the early Eocene at Río Turbio, Santa Cruz (42, 43), antedating the appearance of hypsodonty in Notoungulata by 20 million yr. However, we do not yet know when grasses began to dominate biomes. Data from Gran Barranca suggest that the dominance of grass phytoliths is in agreement with the increased pace of ungulate hypsodonty in the late Eocene. Another possible selective factor may have been dust from the volcanic activity documented by the Sarmiento Formation. The oldest hypsodont notoungulates occur in the Gran Barranca member of the Sarmiento Formation, a sedimentary unit characterized by reworked aeolian and ash-fall deposits (33). The predominance of hypsodont taxa occurred at least 4 million yr after the initiation of volcanism, but the amount of volcanic dust would have become important only when drier conditions became more prevalent.

Thus, drying and cooling terrestrial climates would have triggered the dominance of grasses with their abrasive silica; equally, the climate would have introduced wind-blown pyroclastic dust. Both factors may have contributed to the accelerated rates of evolutionary hypsodonty in the late Eocene through the Oligocene Notoungulata. In either case, replacement of lophodont taxa by hypsodont taxa began in the Casamayoran at about 36 Ma and was essentially complete by 31.5 Ma.

Dr. Mario Martín Mazzoni, Profesor de Geologia, Facultad de Ciencias Naturales y Museo de La Plata, Universidad Nacional de La Plata (UNLP), and Investigador Principal del Consejo Nacional de Investigaciones Científicas y Técnicas (CONICET), died of a massive myocardial infarction on October 1, 1999. We thank K. G. Miller, S. Zack, D. Prothero, M. O. Woodburne, A. Wyss, A. Zucol, D. Piperno, and D. Dilcher for their comments. Research was funded by National Science Foundation grants (SBR 93-18942 and DEB 99-07985) to R.F.K. and R.H.M.

[‡‡]Madden, R. H., and Williams, S. H. & Kay, R. F. (1999) in *Programa y Resumenes, Congreso Internacional Evolución Neotropical del Cenozoico,* Academia Nacional de Ciencias and Museo Nacional de Historia Natural, La Paz, Bolivia, May 19–22, 1999, p. 29 (abstr.), and p. 46 (abstr.), respectively.

1. Flynn, J. J. & Swisher, C. C. (1995) in *Geochronology, Time Scales, and Global Stratigraphic Correlation,* eds., Berggren, W. A., Kent, D. V., Aubry, M.-P. & Hardenbol, J. (Society for Sedimentary Geology, Tulsa, OK), Special Publ. **54**, pp. 317–333.
2. Flynn, J. J. & Wyss, A. (1998) *TREE* **13,** 449–454.
3. Marshall, L. G., Hofstetter, R. & Pascual, R. (1983) *Paleovertebrata, Mém. Extraord.* 1–93.
4. Patterson, B. & Pascual, R. (1972) in *Evolution, Mammals, and Southern Continents*, eds. Keast, A., Erk, F. C. & Glass, B. (State Univ. of New York Press, Albany), pp. 247–309.
5. Simpson, G. G. (1940) *Proc. Am. Philos. Soc.* **83,** 649–709.
6. Simpson, G. G. (1941) *Am. Mus. Novitates* **1120,** 1–15.
7. Spalletti, L. A. & Mazzoni, M. (1977) *Obra Centen., Mus. de La Plata* **4,** 261–283.
8. Spalletti, L. A. & Mazzoni, M. (1979) *Rev. Asoc. Geol. Argentina* **34,** 271–281.
9. Cifelli, R. L. (1985) *Am. Mus. Novitates* **2820,** 1–26.
10. Bond, M., López, G. & Reguero, M. (1996) *J. Vert. Paleontol.* **16**.
11. Wyss, A., Flynn, J. J., Norell, M., Swisher, C. C., Novacek, M., McKenna, M. C. & Charier, R. (1994) *Am. Mus. Novitates* **3098,** 1–31.
12. Marshall, L. G., Cifelli, R. L., Drake, R. E. & Curtis, G. H. (1986) *J. Paleontol.* **60,** 920–951.
13. Kay, R. F., Madden, R. H., Mazzoni, M., Vucetich, M. G., Ré, G., Heizler, M. & Sandeman, H. (1999) *Am. J. Phys. Anthropol. (Suppl.)* **28,** 166 (abstr.).
14. Oviedo, E. (1989) MAG88*: Un sistema de computación para el análisis de datos paleomagnéticos. Su aplicación al estudio paleomagnetico de sedimentos cretácicos de la Cuenca Neuquina* (Universidad de Buenos Aires, Buenos Aires, Argentina).
15. Zijderveld, J. D. A. (1967) in *Methods in Paleomagnetism*, eds. Collinson, D. W., Creer, K. M. & Runcorn, S. K. (Elsevier, Amsterdam), pp. 254–286.
16. Kirschvink, J. L. (1980) *Geophys. J. R. Astron. Soc.* **62,** 699–718.
17. Valencio, D. A., Vilas, J. F. & Mendia, J. (1977) *Geophys. J. R. Astron. Soc.* **51,** 50–74.
18. Berggren, W. A., Kent, D. V., Swisher, C. C. & Aubry, M.-P. (1995) in *Geochronology, Time Scales, and Global Stratigraphic Correlation*, eds., Berggren, W. A., Kent, D. V., Aubry, M.-P. & Hardenbol, J. (Society for Sedimentary Geology, Tulsa, OK), pp. 129–212.
19. Sempere, T., Butler, R. F., Richards, D. R., Marshall, L. G., Sharp, W. & Swisher, C. C. (1997) *Geol. Soc. Am. Bull.* **109,** 709–727.
20. Marshall, L. G., Sempere, T. & Butler, R. F. (1997) *J. South Am. Earth Sci.* **10,** 49–70.
21. Wyss, A., Flynn, J. J., Norell, M., Swisher, C. C., Charier, R., Novacek, M. & McKenna, M. C. (1993) *Nature (London)* **365,** 434–437.
22. Marenssi, S. A., Reguero, M. A., Santillana, S. N. & Vizcaíno, S. F. (1994) *Antarct. Sci.* **6,** 3–15.
23. Case, J. A., Woodburne, M. O. & Chaney, D. S. (1988) *Geol. Soc. Am. Mem.* **169,** 505–521.
24. Woodburne, M. & Case, J. (1996) *J. Mammal. Evol.* **3,** 121–162.
25. Zinsmeister, W. J. (1976) *Antarct. J. U. S.* **11,** 222–225.
26. Zinsmeister, W. J. (1979) in *Historical Biogeography, Plate Tectonics, and the Changing Environment*, eds. Gray, J. & Boucot, A. J. (Oregon State Univ. Press, Corvallis, OR), pp. 349–355.
27. Hall, A. (1977) *Nature (London)* **267,** 239–241.
28. Wrenn, J. H. & Hart, G. F. (1988) *Geol. Soc. Am. Mem.* **169,** 321–447.
29. Lawver, L. A. & Gahagan, L. M. (1998) in *Tectonic Boundary Conditions for Climate Reconstructions*, eds. Crowley, T. J. & Burke, K. C. (Oxford Univ. Press, Oxford), pp. 212–223.
30. Miller, K. G., Wright, J. D. & Fairbanks, R. G. (1991) *J. Geophys. Res.* **96,** 6829–6848.
31. Wilson, G. S., Roberts, A. P., Verosub, K. L., Florindo, F. & Sagnotti, L. (1998) *Bull. Geol. Soc. Am.* **110,** 35–47.
32. Sloan, L. C. & Barron, E. J. (1992) in *Eocene-Oligocene Climatic and Biotic Evolution*, eds. Prothero, D. R. & Berggren, W. A. (Princeton Univ. Press, Princeton, NJ), pp. 202–217.
33. Mazzoni, M. M. (1979) *Rev. Assoc. Arg. Min. Petrol. Sed.* **10,** 33–53.
34. Miller, K. G. (1992) in *Eocene-Oligocene Climatic and Biotic Evolution*, eds., Prothero, D. R. & Berggren, W. A. (Princeton Univ. Press, Princeton, NJ), pp. 160–177.
35. Miller, K. G., Fairbanks, R. G. & Mountain, G. S. (1987) *Paleoceanography* **2,** 1–19.
36. Janis, C. M., Scott, K. M. & Jacobs, L. L. (1998) *Evolution of Tertiary Mammals of North America. I. Terrestrial Carnivores, Ungulates, and Ungulate-Like Mammals* (Cambridge Univ. Press, Cambridge, UK).
37. Pascual, R. & Ortiz-Jaureguizar, E. (1990) *J. Hum. Evol.* **19,** 8–23.
38. Shockey, B. J. (1997) *J. Vert. Paleontol.* **17,** 584–589.
39. Stebbins, G. L. (1981) *Ann. Mo. Bot. Gard.* **68,** 75–86.
40. MacFadden, B. J., Campbell, K. E., Cifelli, R. L., Siles, O., Johnson, N. M., Naeser, C. W. & Zeitler, P. K. (1985) *J. Geol.* **93,** 223–250.
41. Coughenour, M. B. (1985) *Ann. Mo. Bot. Gard.* **72,** 852–863.
42. Berry, E. W. (1937) *Johns Hopkins Univ. Studies Geol.* **12,** 91–97.
43. Malumián, N. & Caramés, A. (1997) *J. South Am. Earth Sci.* **10,** 189–201.
44. Kay, R. F., MacFadden, B. J., Madden, R. H., Sandeman, H. & Anaya, F. (1998) *J. Vert. Paleontol.* **18,** 189–199.
45. Food and Agriculture Organization of the United Nations (1985) Plant Production and Protection Series 24 (FAO, Rome).
46. Braun, J. K. (1993) *Special Publication of the Oklahoma Museum of Natural History* (Norman, OK).
47. Reig, O. A. (1987) *Fieldiana, Zool. (n.s.)* **39,** 347–399.